ApJ in press
Preprint typeset using LaTeX style emulateapj v. 11/26/04

arXiv:astro-ph/0612259v1 11 Dec 2006

THE SPATIAL DISTRIBUTION OF THE GALACTIC FIRST STARS II: SPH APPROACH

Chris B. Brook[1,2], Daisuke Kawata[3,4], Evan Scannapieco[5], Hugo Martel[1], and Brad K. Gibson[6]

ApJ in press

ABSTRACT

We use cosmological, chemo-dynamical, smoothed particle hydrodynamical simulations of Milky-Way-analogue galaxies to find the expected present-day distributions of both metal-free stars that formed from primordial gas and the oldest star populations. We find that metal-free stars continue to form until $z \sim 4$ in halos that are chemically isolated and located far away from the biggest progenitor of the final system. As a result, if the Population III initial mass function allows stars with low enough mass to survive until $z = 0$ ($< 0.8 M_{\odot}$), they would be distributed throughout the Galactic halo. On the other hand, the oldest stars form in halos that collapsed close to the highest density peak of the final system, and at $z = 0$ they are located preferentially in the central region of the Galaxy, i.e., in the bulge. According to our models, these trends are not sensitive to the merger histories of the disk galaxies or the implementation of supernova feedback. Furthermore, these full hydrodynamics results are consistent with our N-body results in Paper I, and lend further weight to the conclusion that surveys of low-metallicity stars in the Galactic halo can be used to directly constrain the properties of primordial stars. In particular, they suggest that the current lack of detections of metal-free stars implies that their lifetimes were shorter than a Hubble time, placing constraints on the metal-free initial mass function.

Subject headings: cosmology:theory — galaxy:evolution — galaxy:formation — galaxy:stellar content — stars:abundances

1. INTRODUCTION

The first generation of stars in the Universe are expected to be metal-free. If some of these stars have lifetimes of a Hubble time, metal-free stars would be currently found in the Milky Way. Hunting metal-free stars, i.e., Population III (Pop III) stars, is an important goal of contemporary astronomy, and extensive searches for extremely low-metallicity stars are underway [e.g. The Hamburg/ESO R-process-Enhanced Star (HERES) survey, and the Sloan Extension for Galactic Understanding and Evolution (SEGUE); see Beers & Christlieb 2005 for an overview of past and current surveys]. To date, surveys have been primarily in the solar neighborhood, which has the obvious advantage over the bulge of proximity, as well as lacking the dust extinction and crowding. Searches also target the outer halo, which retains the latter two advantages. Currently, only 12 stars with iron abundances [Fe/H] < -3.5 have been identified (Beers & Christlieb 2005), with the lowest having [Fe/H] $= -5.4$ (Frebel et al. 2005). Thus far, however, there is no report of the detection of a single star that does not contain any metals. Therefore, one crucial question is raised: is the current survey area the right place to look for the metal-free stars?

Recently, Diemand, Madau, & Moore (2005) used high-resolution N-body simulations to trace the positions of the particles contained in the protogalactic halos collapsing from 3.0σ and 3.5σ density perturbations. Tracing particles in 3.0σ perturbations, they found that the density of such particles in the solar neighborhood is three orders of magnitude lower than in the bulge at $z = 0$. Moreover, tracing particles in 3.5σ perturbations leads to even more extreme results, decreasing the number of these particles at the solar radius by almost another order of magnitude. This implies that the Milky Way's bulge is the best place to search for the very oldest stars and their remnants. Therefore, if Pop III and the oldest stars are one and the same, the non-detection of Pop III stars may simply be due to the surveys looking in the wrong place, and future surveys should focus on the bulge region.

However, the link between the oldest stars, metal poor stars, and metal-free Pop III stars is not so straight forward. The largest halos, forming in the greatest density perturbations, can progress their self-enrichment, and produce the next generation of stars, at very high redshift. Combining semi-analytic galaxy formation recipes of Kauffmann et al. (1999) with N-body simulations of galaxy clusters, rescaled to Milky Way mass, White & Springel (2000) showed that the oldest stars are distributed preferentially at small radii, while low metallicity stars (simply assumed to form in the lowest mass halos) lie preferentially at larger radii in the present Milky Way. This effect is driven by the flatter density profile of low σ peaks, compared to high σ peaks as shown, for example, at $z = 12$ in figure 2 of Moore et al. (2005), and assuming the well established galaxy mass-metallicity relation. However, the association of low metallicity stars with low mass halos does not necessarily mean that the earliest stars in these halos formed from primordial material. The low metallicity of dwarf galaxies may be

[1] Département de physique, de génie physique et d'optique, Université Laval, Québec, QC, Canada G1K 7P4
[2] Dept. of Astronomy, University of Washington, Box 351580, Seattle, WA 98195, USA
[3] The Observatories of the Carnegie Institution of Washington, 813 Santa Barbara St., Pasadena, CA 91101
[4] Swinburne University of Technology, Hawthorn VIC 3122, Australia
[5] Kavli Institute for Theoretical Physics, Kohn Hall, UC Santa Barbara, Santa Barbara, CA 93106
[6] Centre for Astrophysics, University of Central Lancashire, Preston, PR1 2HE, United Kingdom

due to factors caused by inefficient star formation Kennicut (1998), feedback driven outflow of the enriched gas, because of their shallow potential well Dekel & Silk (1986), or inflow of low metallicity material (Köppen & Edmunds (1999). This may occur even if the earliest stars in such halos form from (slightly) enriched gas. But these studies [see also an analytical argument by Miralda-Escudé (2000)] do raise the possibility that Pop III stars have a different radial distribution from the oldest stars, i.e. it is possible that low-density, isolated regions may form stars from primordial material at (relatively) low redshift.

To identify the best location to look for Pop III stars, it is necessary to infuse the dark matter structure formation studies employed in White & Springel (2000) and Diemand, Madau, & Moore (2005) with information pertaining to the metal enrichment of the intergalactic medium. In Scannapieco et al. (2006) (hereafter Paper I), we combined a high-resolution N-body simulation of the formation of the Milky Way with a semi-analytic model of metal enrichment. This model traced the outflows induced by star formation in the collapsing halos identified in the N-body simulation, and tagged the metal-free star particles that were born in halos massive enough to make stars, but isolated enough to not have been enriched by outflows from neighboring halos. We found that Pop III stars were formed over a large redshift range, that peaked at $z \approx 10$, but continued to form down to $z \approx 5$. Tracing these particles to their final locations at $z = 0$, we found that the Pop III distribution covered a wide range of galactocentric radii.

A limitation of this approach, however, is the assumption used for tracing baryonic matter, with the density profile of stellar matter assumed to be the same as that for the dark matter. In this paper (Paper II), we use a different approach: chemo-dynamical simulations. Continued advances in computer technology and numerical methods have made it possible to calculate the dynamical and chemical evolution of disk galaxies self-consistently (e.g. Bekki & Chiba 2001; Abadi et al. 2003; Nakasato & Nomoto 2003; Brook et al. 2004; Steinmetz & Muller 1995; Scannapieco et al. 2005). Such chemo-dynamical simulations can tell us the location of stars with different metallicities and ages at different redshifts. In this paper, we use such information from cosmological chemo-dynamical simulations of Milky-Way analogues to study the birthplace and final distribution of the zero-metallicity stars as well as very old stars. While working at a somewhat lower resolution than in Paper I, this approach nevertheless has the advantage of self-consistently tracing the details of star formation and metal enrichment within dynamical, hierarchical structure formation. In particular, we examine four simulations of Milky-Way-type galaxies which employ various implementations of supernovae (SNe) feedback, different resolutions, and different random initial density fluctuations. Interestingly, we find that the resulting distributions of the oldest and zero-metallicity stars are consistent among the four simulations, robust within our different models.

In §2 we introduce the code and models which we employ. In §3 we show the star formation histories of the zero-metallicity "metal-free" stars. We then show the distribution of such stars, as well as the distribution of very "oldest" stars, the earliest stars forming in each simulation. A summary of our results and our conclusions follow in §4.

2. METHOD

2.1. *The Disk Galaxy Simulation Models*

We simulate four Milky-Way-analogue galaxies using the chemo-dynamical software GCD+, which self-consistently models the effects of gravity, gas dynamics, radiative cooling, and star formation (Kawata & Gibson 2003). Two of the models, AFM and TFM, have identical initial conditions but different prescriptions for modeling the SNe feedback. The other two models, KGCD and AGCD, are higher resolution disk galaxy formation models used in Bailin et al. (2005). We apply the same analysis for all four models with varying evolution histories, prescriptions of star formation and supernovae (SNe) feedback, in order to test the robustness of our conclusions.

All models adopt Λ-dominated CDM cosmological simulations that use the multi-mass technique to self-consistently model the large-scale tidal field, while simulating the galactic disk at high resolution. The initial conditions used for AFM and TFM corresponds to galaxy D1 of Kawata, Gibson, & Windhorst (2004), but in this simulation, we set the high-resolution region to be 8 times the virial radius of this galaxy at $z = 0$. The initial condition of AFM, TFM, and KGCD are constructed with `GRAFIC2` (Bertschinger 2001) and that of AGCD is the same as Abadi et al. (2003) which is kindly provided by M. Steinmetz. All initial conditions have been shown to lead to disk galaxies. Detail description about these models is seen in these earlier papers. Here, we provide a brief description of these models.

In TFM, KGCD, and AGCD, we employ the exactly same recipe as Kawata & Gibson (2003). In these models, 10^{50} erg energy is fed back as thermal energy from each SN, and energy from SNe II and SNe Ia is smoothed over surrounding gas particles according to SPH kernel, in the form of thermal energy, as in Katz (1992). This SNe feedback model is often called thermal feedback model. On the other hand, AFM adopts the adiabatic feedback model introduced in Brook et al. (2004). In this model, to maximize the effect of SNe feedback, we assume 10^{51} erg energy per SN. In addition, gas within the SPH smoothing kernel of SNe II explosions is prevented from cooling. This adiabatic phase is assumed to last for the lifetime of the lowest mass star that ends as a SN II, i.e., the lifetime of 8 $M_\odot$ star (~ 100 Myr). The energy released by SNe Ia, which do not so closely trace the starburst region, is not assumed to have an adiabatic phase.

Thus, with our four models we have three different random seed initial conditions, with two different feedback formalisms, and run at three different resolutions. Table 1 summarizes the parameters of all the simulations. All the models assume the Salpeter initial mass function (IMF) with the mass range of $0.1-60\ M_\odot$. If the IMF for early generation stars are different from the conventional Salpeter IMF, with more massive stars as suggested in the numerical simluations, the total effect of SNe feedback may be stronger than in our simulations. This may reduce the number of the old and/or metal-free stars. Therefore, the absolute mass density of these stars in our simulations needs to be taken with caution. How-

ever, the main aim of this study is to identify the best place to look for the metal-free stars, if they still exist. Thus the important result we want to highlight is the radial distribution rather than the absolute density of the metal free stars. This aspect of our result will only be invalidated if the increased feedback were to greatly effect the enrichment of the IGM, such that isolated halos form from pre-enriched rather than primordial material. In the parameter space survey in Paper I, the strength of that approach was its ability to probe this aspect of the problem for a large range of feedback energies, assuming a variety of top heavy IMFs, and this gives us confidence. Under these assumptions, we can study the expected distribution of the the metal-free stars in the Milky Way at $z = 0$, if they had a similar IMF as the local stars.

2.2. *Identifying Metal-Free Stars*

In Paper I, we combined a high-resolution N-body simulation that can resolve the formation of halos $\sim 10^7 M_\odot$ with a semi-analytic model of outflows. In our semi-analytic model, we considered that the outflows are induced by star formation in the halos, depending on their total mass, and traced the enrichment history of the intergalactic medium due to such outflows. Then, we identified the site of metal-free star formation as halos which are massive enough to make stars and have not been enriched by the outflows from other halos.

It is also worth mentioning that numerical simulations have shown that outflows tend to be highly anisotropic, even if they originate from spherical halos (Martel & Shapiro 2001a,b). The external medium surrounding halos tends to be anisotropic. When gas ejected from halos enters that medium, it naturally follows the path of least resistance, becoming anisotropic. Energy and metals are deposited in low-density regions, away from dense structures. This effect strongly reduces the likelihood of galaxies being hit by outflows originating from other galaxies, unless the outflows are very narrow and can travel large distances, across cosmological voids (Pieri, Martel, & Grenon 2006). The net effect is a significant suppression of the metal-enrichment of halos by neighboring galaxies, enabling these halos to retain their primordial composition up to low redshifts, when they may form stars.

The chemo-dynamical simulations employed in this present study do not require the inclusion of an approximate semi-analytic model. Rather, they include the effects of the SNe feedback completely self-consistently within the SPH method. First-generation star particles form on an individual basis, and we track the independent chemical evolution of each and every gas particle, starting from primordial gas. We then use these individual metal-free star particles as tracers of metal-free stars, and analyze their locations at $z = 0$.

It is believed that the bulk of metal-free stars are formed in halos with total mass around $\sim 10^7 M_\odot$ (Tegmark et al. 1997; Fuller & Couchman 2000; Yoshida et al. 2003). However, it is unknown what fraction of the gas in the halo turns into metal-free stars (e.g. Abel, Bryan, & Norman 2000), whether the SNe by metal-free stars disrupt the gas in the halo completely (Bromm, Yoshida, & Hernquist 2003), although full radiative transfer calculations of Kitayama & Yoshida (2005) indicate that all the gas is evacuated, or whether such SNe also induce the second generation stars in the halo (Susa & Umemura 2006). It is also possible that two types of metal free stars form, Pop III stars, with mass of $100 M_\odot$ and more, and metal free stars forming in halos with T$> 10^4$K, with masses as low as $10 M_\odot$ (Greif & Bromm 2006). Simulations of these processes have far greater resolution than we can manage when simulating a galaxy in a cosmological context.

Unfortunately, the resolution of cosmological, SPH galaxy formation simulations is not sufficient to identify the halos where the metal-free stars are likely to form, or to follow the physical processes in the halos, in the manner of e.g. Yoshida (2006). Rather, the minimum mass of the halo that we can resolve is between $10^8 M_\odot$ and $10^9 M_\odot$, depending on the simulation. However, in a hierarchical clustering scenario, each and every $10^8 M_\odot - 10^9 M_\odot$ halo is expected to be pre-dated by smaller halos, i.e. building blocks. Thus, if a given $\approx 10^8 - 10^9 M_\odot$ halo is sufficiently isolated, its earliest forming smaller progenitor, such as $\sim 10^7$ M$_\odot$ halos, should have been the site of metal-free star formation. Based on this scenario, we assume that some fraction of the mass of simulation metal-free star particles is metal-free stars, and that the metal free simulation star particle trace the location of the metal-free stars. Thus our study assumes that the final distribution of stars in the stellar halo is primarily determined by the dynamics and accretion of the $\sim 10^8$M$_\odot$ halos that our simulations resolve. In this case the remaining uncertainty is how many "metal-free stars" correspond to each zero metallicity star particle at $z = 0$. As mentioned above, this depends on the star formation history in the $10^6 - 10^7$M$_\odot$ mini-halos which we do no resolve. We simply assume an upper limit, by assuming all the stars in that simulation star particle are metal-free, and follow the Salpeter IMF. This assumption guarantees that some fraction of metal-free stars survive till z=0, and allows us to use the metal-free simulation star particles as tracers of the positon of metal-free stars. Therefore, our absolute mass density of the metal-free stars are likely overestimated. However, we are able to determine the radial distribution of the metal-free stars, using this simple approach. This allows us to determine whether local observations can be used as a constraint on the Population III IMF.

Finally, we also trace the position of old stars, which we define as the oldest star particles, regardless of whether they form from primordial material. In order to compare their distributions with metal-free stars, the mass of oldest and metal-free stars that we trace are approximately equal, i.e. the total mass of the oldest star particles and metal-free star particles are the same. As mentioned above, we employ four disk galaxy formation models, that adopt different galaxy formation models and different prescriptions of SNe feedback. These test how the final distribution of metal-free stars and the oldest stars are sensitive to the evolution history of galaxies and the effect of the SNe feedback. Hereafter, we call the simulation star particles that house metal-free stars, i.e. first-generation Pop III stars, and an equivalent mass of the very oldest star particles as "oldest" stars.

The strengths and shortcomings of the SPH approach, which includes gas dynamics, cooling, star formation and feedback self consistently (Paper II), and the higher reso-

TABLE 1
Parameters of the simulations

Model	$M_{\rm vir}$ ($M_\odot$)	$r_{\rm vir}$ (kpc)	$m_{\rm gas}$[a] ($M_\odot$)	$m_{\rm DM}$[b] ($M_\odot$)	$\epsilon_{\rm gas}$[c] (kpc)	$\epsilon_{\rm DM}$[d] (kpc)	Ω_0	Λ_0	h_0	Ω_b	σ_8
AFM	$10.\times10^{11}$	275	7.3×10^6	4.9×10^7	0.93	1.6	0.3	0.7	0.7	0.039	0.9
TFM	4.9×10^{11}	275	7.3×10^6	4.9×10^7	0.93	1.6	0.3	0.7	0.7	0.039	0.9
KGCD	8.8×10^{11}	240	9.2×10^5	6.2×10^6	0.57	1.1	0.3	0.7	0.7	0.039	0.9
AGCD	9.3×10^{11}	270	3.3×10^6	1.9×10^7	0.87	1.5	0.3	0.7	0.65	0.045	0.9

[a]Mass of gas particles.
[b]Mass of dark matter particles.
[c]Softening length of gas particles.
[d]Softening length of dark matter particles.

lution N-body + semi-analytic approach, which allows a greater diversity of feedback implementations (Paper I) make the two studies complimentary. Reading the two together allows us to gain greater confidence in our results.

3. RESULTS

In Figure 1, we plot the star formation rate (SFR) as a function of redshift for our four simulated Milky-Way analogues. The SFR for all stars within the virial radius at $z = 0$ is plotted as a dot-dashed line, and the SFR for metal-free stars as a solid line. It is notable that the AFM and TFM models, which have the same initial conditions but different treatments of SNe feedback, have significantly different star formation histories, with star formation relatively delayed in the AFM run (see Brook et al. 2004, for details).

Metal-free stars continue forming over a wide range of redshifts, from before redshift $z = 11$ down beyond redshift $z = 4$. Even though it had a relatively large effect on the star formation history of the galaxy, the different feedback implemented in the AFM and TFM runs have not resulted in a drastic change in the star formation history of metal-free stars. Although the AFM, KGCD, and AGCD form very few metal-free stars after redshift $z = 4$, metal-free stars do continue to form beyond redshift $z = 3$. Overall, the redshift range of metfree star formation is quite consistent among the four models, starting along with the oldest stars beyond redshift $z = 11$ and continuing to $z \sim 3$. Furthermore, this redshift range is roughly consistent with the weak and intermediate wind models in Paper I. As expected with the differences between the models explained above, the higher resolution simulations in Paper I allow some metal-free stars to form at higher redshift, $z \sim 15$.

Figures 2–5 present the final distributions of both metal-free and oldest stars. The top left panels show the distribution of the oldest (red "×") and metal-free (black "+") stars in X-Z plane, with axis of 100 kpc, and where Z is the direction of the rotation axis of the stellar disk at $z = 0$. The upper right panels show the mass density of the two populations as a function of radius (distance from the center), in units of $M_\odot/{\rm pc}^3$. The stellar halo mass of each simulation is normalized to that of the Milky Way, by requiring that the solar neighborhood density matches that for the Milky Way, 5.7×10^5 $M_\odot{\rm pc}^{-3}$ (Preston, Shectman, & Beers 1991).

The lower left panel of figures 2–5 show the radial dependence of the mass fraction of metal-free and oldest stars with respect to the total stellar mass at each radius at $z = 0$. The lower right panel displays the distributions of the radius of the birth-place for metal-free stars and oldest stars, which is measured from the center of the largest proto-galaxy at the time they born.

Although the details of the distribution of metal-free and oldest stars differ among the four models, several trends can be seen to be common to all models. Not surprisingly, the absolute density of metal-free and oldest stars are higher at smaller radii. The oldest stars have steeper density profile than metal-free stars, i.e. oldest stars are more centrally concentrated. In terms of where these stars are best searched for in current surveys of stars, the most important quantity is not the absolute density, but rather the number fraction, with respect to the field stars. This is shown in the lower left panels of Figures 2–5. Here, we define the field stars as all stellar halo stars at that radius, computed by using the Toomre diagram and requiring that $T^2+V^2 > (V-V_{\rm disk})^2$ where $T^2 = U^2 + W^2$, U, V, W are the radial, rotational, and out-of-plane velocity components, respectively, and $V_{\rm disk}$ is the rotation velocity of the stellar disk component. Here, $V_{\rm disk}$ for each model is measured as the mean rotation velocity for the young disk stars (which formed after $z \sim 0.8$)

These panels show clearly that the oldest stars are highly concentrated in the bulge regions in the center of the galaxies. On the other hand, metal-free stars have a higher fraction in the outer regions, i.e. in halo region. This strong difference between the oldest and the metal-free stars is in fact more extreme than what was seen in Paper I (see Figs. 4, 5, and 7 in that paper). In Paper I, our N-body+semi-analytic model predicted a roughly constant fraction independent of the radius, while the chemo-dynamical simulation model shown here predicts that the outer region has a higher fraction of metal-free stars than the inner region. This is because the chemo-dynamical simulations naturally provide the density profile of the field stellar component, which is more centrally concentrated than the dark matter component. This difference leads to a difference in the profiles of the normalized mass fraction of metal-free stars in our two papers. Nevertheless, if anything our conclusion from the chemo-dynamical models is even stronger than that reached in Paper I, and we predict that the current survey area, i.e. the solar neighborhood and outer halo,

TABLE 2
Average baryonic mass of the proto-galaxies where metal-free stars and oldest stars form (in units of $10^9 M_\odot$).

Model	metal-free stars	oldest stars
AFM	1.5	6.5
TFM	1.3	6.8
KGCD	0.7	8.2
AGCD	2.1	4.3

is the best place to look for Pop III stars. Thus, from a completely different perspective, we again find that *if they have sufficiently long lifetimes, a significant number of stars formed in initially primordial gas should be found in the Galactic halo.*

While this overall trend is constant across our SPH models, there are nevertheless a number of interesting differences between the runs, which we now discuss in further detail. First, we compare the TFM and AFM runs, i.e., the runs with different implementations of SNe feedback. Figures 2 and 3 show that both metal-free and oldest stars are slightly more centrally concentrated in TFM model than the AFM model. This is related to their star formation histories in Figure 1. In TFM, a larger number of stars are born at very high redshifts, because there is no mechanism to suppress star formation in the small proto-galaxies. As a result, oldest stars in the TFM run are an older population than those in the AFM run, and there is a larger fraction of metal-free stars which are oldest stars, "metal-free+oldest stars." Due to the so-called bias effect, the halos near the density peak of the final system form earlier, and the metal-free+oldest stars form in these halos. The lower-right panels of Figures 2 and 3 demonstrate this clearly. In TFM, more metal-free stars form close to the center of the biggest galaxy, which leads to the bimodal distribution of the distance of their birth place. The stars which formed close to the center of the biggest galaxy accreted to the system at earlier epoch. This leads to a larger number of metal-free +oldest stars ending up in the central region in TFM than AFM.

KGCD has the most clear difference in distributions between metal-free and oldest stars, in terms of their mass fraction at different radii, with the model AGCD also showing a distinct difference in such distributions. In the bottom right panels of Figures 2–5, the largest progenitor is taken as being at the lowest radius. Examining the AGCD model for example, this diagram highlights how a relatively small number of metal-free stars can pollute the progenitor in which many of the oldest stars form. Yet at large distances from this largest, central progenitor, metal-free stars continue to form.

Three different initial conditions having three different patterns of small-scale density perturbations have been employed in our models, which lead to different merger histories of their progenitor halos, i.e., building blocks. Yet all models have similar spreads in the distribution of oldest stars, with a cutoff of the oldest stars around 10 kpc. Lower panels of Figures 2–5 show how the final distribution of metal-free and oldest stars reflects their birth places. The oldest stars generally form in the largest progenitor, associated with the largest density peak, collapsing at the highest redshift, so that they tend to be in the inner region of the galaxy at $z = 0$. Even though the final distributions of metal-free and old stars depend to a degree on their merger histories, all the models lead to similar trends for the distributions of metal-free and oldest stars.

Although our chemo-dynamical simulations are not capable of resolving the minimum mass of halos which can form metal-free stars, $\sim 10^7\ M_\odot$, it is still interesting to see the mass of the halo in which metal-free and oldest stars formed. Using a friend of friends (FOF) algorithm at each time-step, we are able to calculate the mass of the halos in which each star is born. We are limited here by time resolution of the simulation outputs, where we need to assume that the mass of an object has not changed significantly between the output time steps, ~ 0.2 Gyr. Table 2 presents the mean total masses of halos in which metal-free and oldest stars formed, respectively, where we define the total mass of the halo as a total (dark matter and baryon) mass within the halo found by our FOF algorithm. It is clear that the masses of the halos where metal-free stars form are on average lower than those of halos where oldest stars form. This ranges from a factor of ~ 2 larger in the AGCD simulation to a factor of ~ 12 in the higher-resolution KGCD simulation. Combined with the radial distribution of the birth-places of the metal-free stars, shown in Figures 2–5, it is clear that metal-free stars form in lower mass halos that collapse at later epochs, but are chemically isolated from the more massive, earlier collapsing halos in which the oldest stars are born. Consequently, metal-free stars have a much greater spread in distribution, compared with oldest stars.

4. SUMMARY AND CONCLUSIONS

Using chemo-dynamical simulations of Milky-Way-analogue galaxies, we study the present day distribution of stars formed from primordial material, i.e., first-generation stars ("metal-free stars"), and an equivalent mass of the very earliest stars formed ("oldest stars"). Our simulations employ various implementations of energy feedback, different resolutions, and different random initial density fluctuations. We find consistent trends in the distributions of the metal-free and oldest stars in our four diverse simulations at least withing the limitations of our modeling. The main results are as follows:

- Metal-free stars can form in isolated proto-galaxies until relatively low redshift. Therefore, metal-free stars are not necessarily among the very oldest stars.
- Metal-free stars have different radial distribution profiles from oldest stars. The oldest stars have a more centrally concentrated distribution, i.e., they are preferentially found in the bulge regions of the Milky Way. On the other hand, metal-free stars are distributed through the halo, and in terms of the fraction with respect to the field stars, metal-free stars are easier to be found in the outer regions.

In addition, our chemodynamical simulation approach suggests:

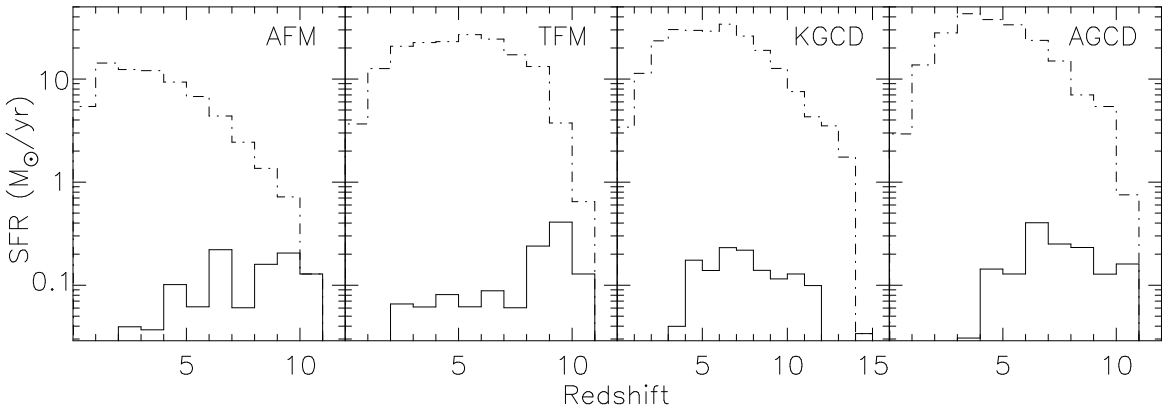

FIG. 1.— Star formation rates (SFR) in $M_\odot$/yr for the 4 models, from left to right: AFM, TFM, KGCD, and AGCD. The dot-dashed line shows all stars, while the solid line shows the SFR for stars formed from primordial material, or "metal-free" stars.

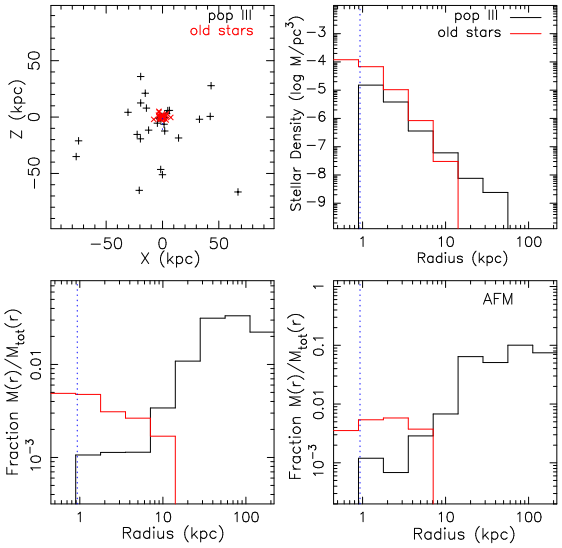

FIG. 2.— The distribution of the oldest (red "×") and metal-free (black "+") stars in the AFM are plotted in X-Z plane in the top left panel, with axis of 100 kpc, and where Z is the direction of the angular momentum vector. The oldest stars are centrally concentrated in the bulge region, while the metal-free stars are spread throughout the halo. In the last three panels, red lines show the oldest stars while black lines are metal-free stars. The blue dotted line indicates the spatial resolution limitation of the simulations. The upper right panel shows the mass density of the two populations as a function of radius, in units of $M_\odot/\mathrm{pc}^3$. The stellar halo density of the simulation is normalized to that of the Milky Way in the solar neighborhood. Stellar mass loss from a top heavy IMF is also not accounted for. The lower left panel shows the radial dependence of the mass fraction of stars at $z = 0$, for the two populations. The lower right panel shows the radial dependence of the mass fraction of the two populations of stars at their birth-place and birth-time. For this plot, the center at each time is taken as the center of the largest protogalaxy at that time.

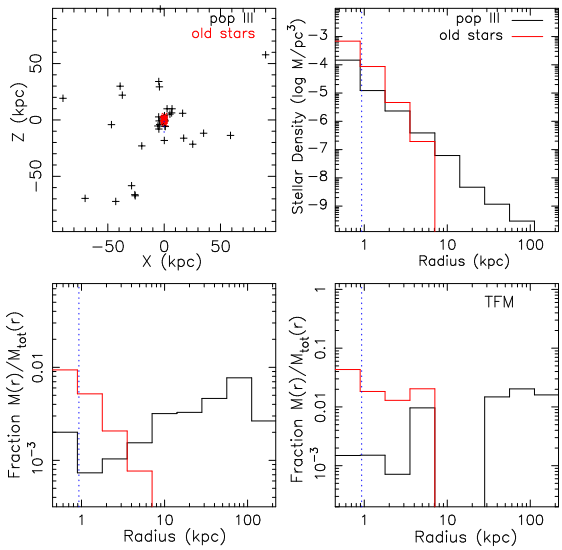

FIG. 3.— Same as Figure 2, for the TFM. No significant difference in trends are apparent, despite the difference in feedback models and subsequent difference in star formation histories .

- The stellar halo density profile has a steeper slope than the dark matter density profile. As a result, the mass fraction of the metal-free stars with respect to the halo stars are higher in the outer region. The almost flat radial trend found in Paper I is due to the assumption that the stellar density profile is the same as the dark matter density profile.

The results are driven by the combination of two results: (1) the contribution of different sigma overdensities have different density profiles in the final halo, ie lower sigma peaks have flatter density profiles (Moore et

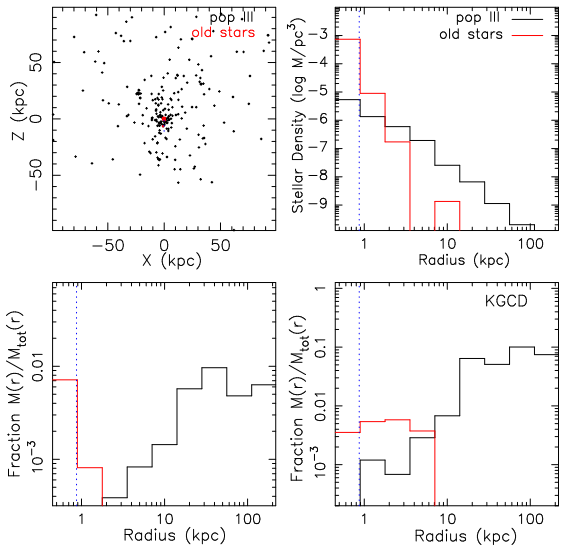

FIG. 4.— Distributions for KGCD model, using the formats of the previous two figures.

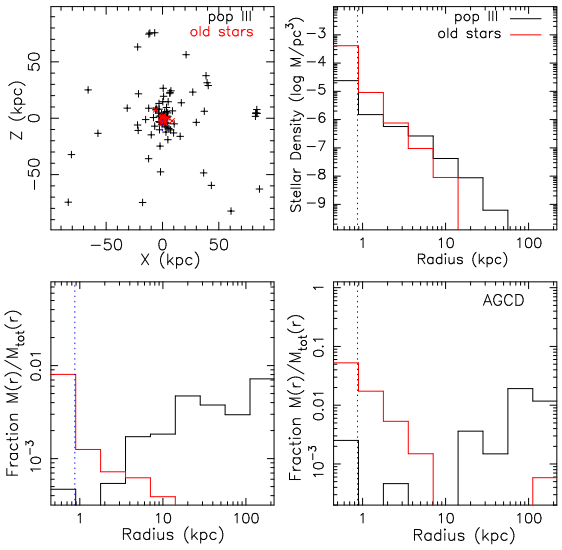

FIG. 5.— Distributions for AGCD model, using the formats of the previous three figures.

al 2006), and the fact that the isolated, relatively late forming proto-galaxies (i.e. those forming in low sigma peaks), form from primordial material.

In terms our question "where are the metal-free stars?", our chemo-dynamical simulation approach has reached the same answer as Paper I. Thus, we repeat here our conclusion in Paper I: if they have sufficiently long lifetimes, a significant number of stars formed in initially primordial star clusters should be found in the Galactic halo. This means that there is no compelling theoretical reason to motivate observational searches in more difficult environments, i.e., in the bulge region, and present observations should be taken as directly constraining the distribution of Population III (Pop III) stars. The lack of metal-free halo stars today should be taken as strong evidence of a $M \geq 0.8\ M_{\odot}$ lower limit on the IMF of metal-free stars. Our results provide encouragement for observers of extreme low-metallicity stars in the solar neighborhood, which have direct implications on our knowledge of the chemical properties of Pop III stars, and encourage theorists who wish to use such results as the basis of their analysis of the nature of the metal-free stars.

We thank M. Pieri for helpful comments and useful information. We acknowledge the Astronomical Data Analysis Center of the National Astronomical Observatory, Japan (project ID: wmn14a), the Institute of Space and Astronautical Science of Japan Aerospace Exploration Agency, the Australian and Victorian Partnerships for Advanced Computing, and the Laboratoire d'Astrophysique Numérique, Université Laval. CB and HM are supported by the Canada Research Chair program and NSERC. DK thanks the JSPS for financial support through a Postdoctoral Fellowship for research abroad. ES is supported by the National Science Foundation under grant PHY99-07949.

REFERENCES

Abadi, M. G., Navarro, J. F., Steinmetz, M., & Eke, V. R. 2003, ApJ, 591, 499
Abel, T., Bryan, G. L., & Norman, M. L. 2000, ApJ, 540, 39
Bailin, J. et al. 2005, ApJ, 627, L17
Beers, T. C., & Christlieb, N. 2005, ARA&A, 43, 531
Bekki, K., & Chiba, M. 2001, ApJ, 558, 666
Bromm, V., Yoshida, Y., & Hernquist, L. 2003, ApJ, 596, L135
Brook, C. B., Kawata, D., Gibson, B. K., & Flynn, C. 2004, MNRAS, 349, 52
Dekel, A. & Silk, J. 1986 ApJ, 303, 39
Diemand, J., Madau, P., & Moore, B. 2005, MNRAS, 364, 367
Köppen & Edmunds 1999 MNRAS, 306, 317
Frebel, A. et al. 2005, Nature, 434, 871
Fuller, T. M., & Couchman, H. M. P. 2000, ApJ, 544, 6
Greif, T. H., & Bromm, V. 2006, submitted to MNRAS (astro-ph/0604367)
Katz, N. 1992, ApJ, 391, 502
Kawata, D., & Gibson, B. K. 2003, MNRAS, 340, 908
Kauffmann, G., Colberg, J. G., Diaferio, A., & White, S. D. M. 1999, MNRAS, 303, 188
Kennicut, R. C., 1998 ApJ 498, 541
Kitayama, T. & Yoshida, N. 2005, ApJ, 630, 675
Martel, H., & Shapiro, P. R. 2001a, Rev.Mex.A&A(SC), 10, 101
Martel, H., & Shapiro, P. R. 2001b, in Relativistic Astrophysics, AIP Conference Proceedings 586, eds. J. C. Wheeler & H. Martel, p. 265
Miralda-Escudé, J. 2000, in The First Stars, MPA/ESO Workshop, eds. A. Weiss, T. G. Abel, & V. Hill, Springer-Cerlag, p. 242
Moore, B., Diemand, J., Madau, P., Zemp, M., & Stadel, J. 2005, MNRAS, 368, 563
Nakasato, N., & Nomoto, K. 2003, ApJ, 588, 842
Pieri, M., Martel, H., & Grenon, C. 2006, submitted to ApJ (astro-ph/0606423)
Preston, Shectman, Beers, 1991, ApJ, 375, 121
Scannapieco, C., Tissera, P. B., White, S. D. M., & Springel, V. 2005, MNRAS, 364, 552
Scannapieco, E., Kawata, D., Brook, C. B., Schneider, R., Ferrara, A., & Gibson, B. K. 2006, submitted to ApJ (Paper I)
Steinmetz, M., & Muller, E. 1995, MNRAS, 276, 549
Susa, H., & Umemura, M. 2006, submitted to ApJ (astro-ph/0604423)
Tegmark, M., Silk, J., Rees, M. J., Blanchard, A., Abel, T., & Palla, F. 1997, ApJ, 474, 1
White, S. D. M., & Springel, V. 2000, in The First Stars, MPA/ESO Workshop, eds. A. Weiss, T. G. Abel, & V. Hill, Springer, p. 327
Yoshida, N., Abel, T., Hernquist, L., & Sugiyama, N. 2003, ApJ, 593, 645
Yoshida, N. 2006 NewAR, 50, 19